

NANO EXPRESS

Open Access

Electric Field-Controlled Crystallizing CaCO₃ Nanostructures from Solution



Jian Quan Qi^{1,2*}, Rui Guo¹, Yu Wang², Xuan Wen Liu¹ and Helen Lai Wah Chan²

Abstract

The role of electric field is investigated in determining the structure, morphology, and crystallographic characteristics of CaCO₃ nanostructures crystallized from solution. It is found that the lattice structure and crystalline morphology of CaCO₃ can be tailored by the electric field applied to the solution during its crystallization. The calcite structure with cubic-like morphology can be obtained generally without electric field, and the vaterite structure with the morphology of nanorod is formed under the high electric field. The vaterite nanorods can be piled up to the petaliform layers. Both the nanorod and the petaliform layer can have mesocrystal structures which are piled up by much fine units of the rods with the size of several nanometers. Beautiful rose-like nanoflowers can be self-arranged by the petaliform layers. These structures can have potential application as carrier for medicine to involve into metabolism of living cell.

Keywords: CaCO₃, Nanoflower, Electric field

Background

Electric field is ubiquitous in nature. It causes the phenomena as great as thunder and lightning or even as fine as the electrostatic interaction among atoms or molecules. It was proposed that the earliest organic compound to biomolecule was produced in the ancient sea on the earth under high electric field, i.e., thunder and lightning [1]. The carbon nanotube was also firstly synthesized by point discharge between two graphite electrodes under high electric field [2]. Now, electric field offers a facility for various controlling technically. Electrospinning is one of the electric field controlled techniques that has gained tremendous attention in the last decade [3, 4] as polymer-processing method for polymer nanofibers [5] and tissue engineering scaffold [6], even as well as to metals and ceramics [7]. Electric field-controlled sintering is also an important method for the fabrication of a textured ceramics. However, the chemical reaction and the crystallization of nanostructures from solution under the electric field are not focused enough. Both of them are associated with the electrostatic force, and thus, the investigation to the

chemical reaction or crystallization in solutions under a certain electric field will be amazing.

CaCO₃ is one of the standard model systems because of its abundance in nature, participation in the formation of a certain geologic structure as Karst cave, association with biological calcium metabolism, its important industrial applications. Crystallization and morphological control of CaCO₃ have attracted extensive attention for decades [8–23]. Much of them focus their attention on surfactant controls. Our study is inspired by the formation of the earliest biomolecule under thunder and lightning, also electrospinning in technology. The polymorphy and morphology of CaCO₃ nanostructures synthesized under the high electric field from solution is investigated and found that they are much different from those without electric field.

Methods

The synthesis system is illustrated in Fig. 1 as our patent described [24]. In a typical synthetic process, 3.52 g Ca(Ac)₂ (BDH Chem. Ltd., UK) was dissolved in 10 ml absolute ethanol (International Laboratory, USA) and then transferred into a syringe as injecta. 2.76 g K₂CO₃ (BDH Chem. Ltd., UK) was dissolved in 200-ml deionized water in a stainless steel vessel as a base solution. The vessel was linked to the ground of high voltage power serving as a counter electrode. The syringe was fixed on

* Correspondence: jianquanqi@mail.tsinghua.edu.cn

¹School of Materials Science and Natural resources, Northeastern University at Qinhuangdao, Qinhuangdao 066004 Hebei Province, People's Republic of China

²Department of Applied Physics and Materials Research Center, The Hong Kong Polytechnic University, Hung Hom, Hong Kong

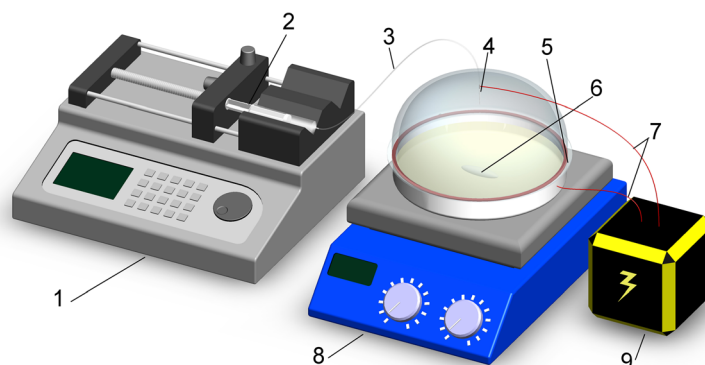


Fig. 1 The illustration of the system for synthesis of nanostructures under electric field: 1 ejector jet pump, 2 syringe, 3 perfusion tube, 4 entry needle, 5 stainless steel vessel, 6 magnetic stirrer, 7 electric wire, 8 magnetic stirring apparatus, and 9 high voltage power

the ejector jet pump. The syringe nozzle was linked to a perfusion tube, which the other end was fixed on an entry needle. The entry needle simultaneously served as an electrode, to which a high electric field of 0–1000 kV/m can be applied, and the distance to the counter electrode is 10–25 cm in our laboratory systems. The injecta solution was injected into the base solution which was stirred quickly by magnetic stirrer. In our experiments, 0 and 8 kV were employed and perfusion flow was fixed at 80 $\mu\text{l}/\text{min}$. After the completion of the perfusion, obtained white slurry was filtered and washed several times by deionized water. Through the vacuum drying, the white as-prepared powders were checked by the X-ray diffraction (XRD, a Philips Diffractometer, X'Pert-Pro MPD), field emission scanning electron microscopy (FE-SEM, JSM6335F NT), and transmission electron microscopy (TEM, a JEOL TEM, JSM2010).

Results and Discussion

CaCO_3 has three anhydrous crystallographic polymorphs: vaterite (the least stable), aragonite, and calcite (the most stable). Vaterite particles do not show well-defined morphologies and usually aggregate into spherical particles. The vaterite form can crystallize in either an orthorhombic or a hexagonal structure. With the aids of surfactants and/or templates, hollow vaterite spheres, micro floret, hexagonal prism vaterite crystalline powders, etc. could be synthesized. There is seldom aragonite in nature. It may be associated with the activity of the creatures on the earth. Among the three polymorphs of CaCO_3 , calcite would be crystallized generally from the solution without outside disturbance because it is the most thermodynamic stable phase.

To clear investigate the effect of electric field on the crystallization of CaCO_3 , two comparable experiments have been done. In our study, both the precipitation of CaCO_3 chemical reactions under 8 kV (~ 800 kV/mm) electrical field and that under electrical field free (0 kV/mm) were

completed in our instrument as described above and named as electric field (EF) sample and electric free (NE) sample, respectively. The XRD patterns are shown in Fig. 2a. It is obviously shown that the main crystal phase of the sample under electric field free is calcite (#pdf:05-0586) as expected. Comparably, the crystal phase of the sample which was fabricated under 8 kV electric field is mainly vaterite (#pdf:33-0268). It is confirmed that vaterite can be synthesized under high electric field, and calcite can be obtained under the condition of electric field free preferentially. In the experiments, there is a little calcite in EF sample except for vaterite as the main phase because applied electric field is not high enough. In comparison with the sample of NE, a little of vaterite are produced due to electrostatic force of the surface tension of the solution which solved acetic salt as surfactant.

The vibrational spectroscopy as Raman spectroscopy is sensitive to the structural transformation; the distortions and defects of lattice cell at the molecular level can be detected [25]. It is a paradigm that the tetragonality of BaTiO_3 can be identified by the Raman spectrum, and the fine distinction on phase structures can be distinguished [26]. It is also a powerful tool to determine the polymorphs of CaCO_3 crystals [27–29]. Figure 2b shows the Raman spectrums of sample EF and NE which representatively identified as vaterite and calcite as the literatures documented [27, 29]. The strongest bands of calcium carbonate polymorphs at around 1100 cm^{-1} overlap, but vaterite has double peaks whereas calcite has mono one. The most intense Raman bands are observed in the low frequency region ($50\text{--}400\text{ cm}^{-1}$), which corresponds to the lattice mode vibrations. In these bands, the characteristic peaks of calcite are strong and narrow, whereas the vaterite bands are large and overlap at 150 and 281 cm^{-1} with calcite. The modes of wide band around 110 and 300 cm^{-1} are the characteristic vibration of vaterite lattice as shown as Fig. 2b.

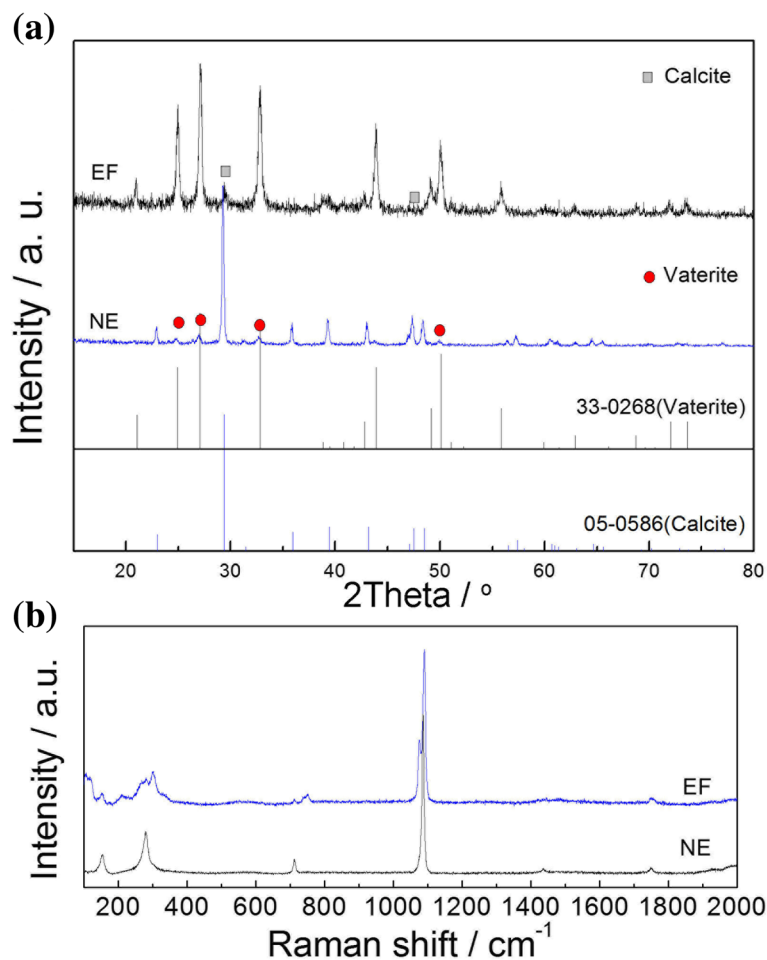


Fig. 2 The XRD pattern and Raman spectra of CaCO_3 synthesized under electric field (EF) and electric free (NE). **a** XRD pattern. **b** Raman spectra

The microstructures of EF sample by SEM are shown in Fig. 3a–d in series. The nanorods with the size of 500 nm in length and 50 nm in diameter are apparently shown in Fig. 3a, which synthesized under the electric field. The nanorods can assemble to petaliform layers as some as shown in Fig. 3b spontaneously. Figure 3b clearly shows the media products of the evolution of nanoflowers. It is amazing that these petaliform layers can assemble further to beautiful rose-like nanoflowers as shown in Fig. 3c, d. The petals of the rose are clearly composed by nanorods in these pictures. All of these reveal the beauty of the crystallography.

The microstructures of NE sample are shown in Fig. 3e, f. There are two morphologies in Fig. 3e, cube and sphere inspect of two phases indexed from XRD pattern, calcite and vaterite. From the point of view of crystallization characteristics of the polymorph, the cube is assigned as calcite and sphere as vaterite. Here, the sphere-like morphology of vaterite is much different from that as flower-like in EF sample, although they both have the same phase as vaterite. The calcite morphology is clearly

shown in Fig. 3f also. The cubes are clearly grown from square layer by layer. It is interesting that the polymorphs can be obtained from the different conditions of the crystallization.

In order to study the characteristics of the crystallization under the electric field, more details of the sample EF was observed by TEM. Figure 4 has shown a much fine structure of a petaliform layer nanostructure of vaterite. Figure 4a shows a petaliform layer uppled by a series of nanorods. Figure 4b shows a conjunction of two nanorods. More detail structure of it is shown in Fig. 4c. It is clearly shown that the nanorods and even the conjunction of them are piled up by much fine units of the rods with the size of 10 nm in length and 3 nm in diameter. Much fine pores with the size of about 5 nm among the units are clearly observed. These structures can have some unique characteristics for absorption or/and filter of special molecules with large specific area. Therefore, our samples have the potential application as a carrier for medicine to get involved in metabolism of living cell.

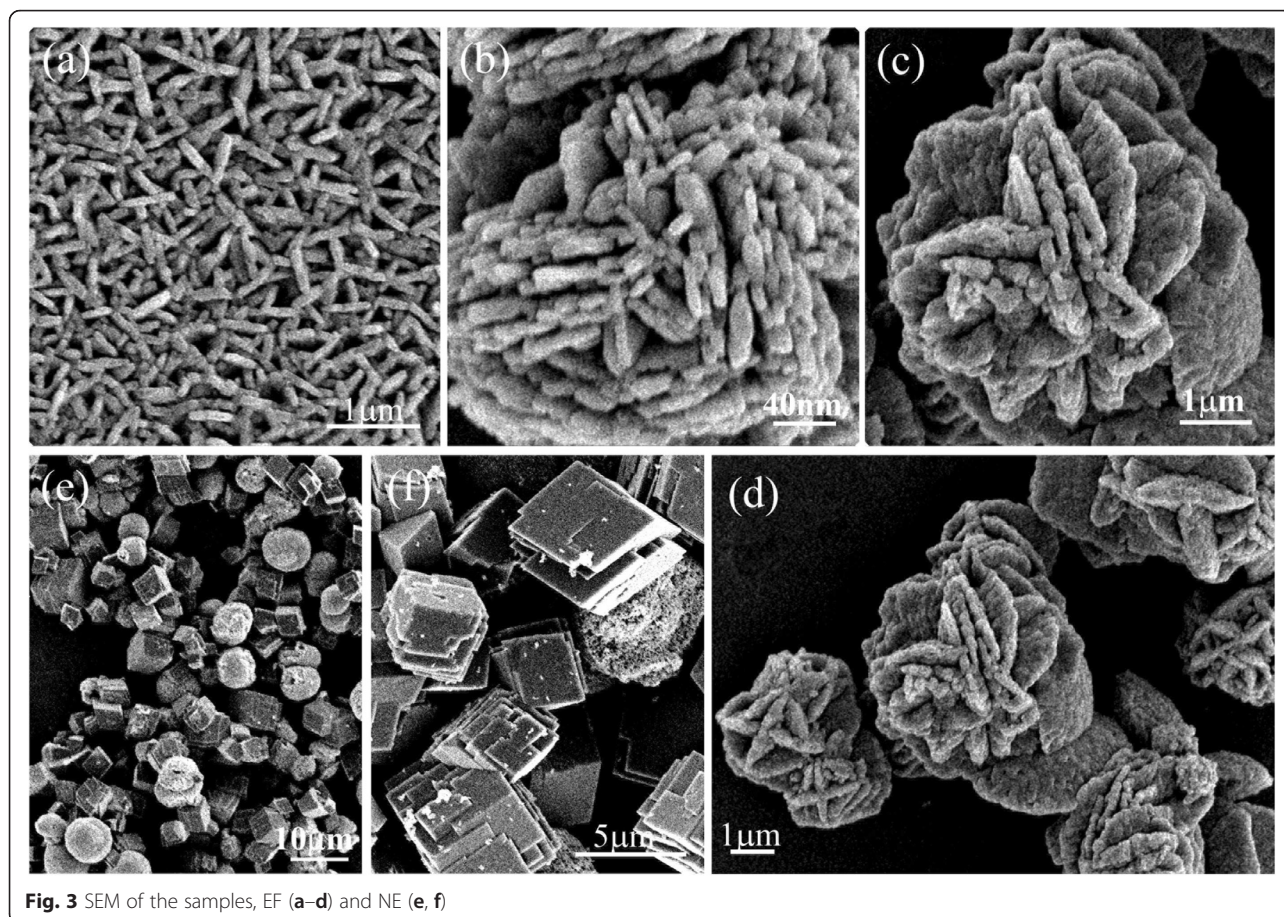


Fig. 3 SEM of the samples, EF (a–d) and NE (e, f)

It is amazing when we check the SEAD of the sample. A series of perfect hexagonal single crystal diffraction pattern is revealed in Fig. 4d. Obviously, the petal of rose-like nanostructure is a single crystal from this point of view and is called as mesocrystals. As documented previously, besides conventional crystallization, there are also nonclassical pathways of crystallization via colloidal intermediates and mesoscale transformation [8–11], in which crystalline structures are constructed and/or transformed from larger units instead of single ions. In addition, crystals can be assembled from nanoscopic building units in an almost perfect three-dimensional orientation to form so-called mesocrystals, exhibiting well-faceted outer surfaces. In the case of inorganic minerals [9, 11, 30], these typically fuse to single crystals, likely as a result of high lattice energy, whereas in organic crystals [31], they can be isolated.

Polarized hydroxyapatite ceramics was used to study the effect of surface electric field on crystallization of calcite. It was found the oriented growth of calcite crystals with the rhombohedra {10.4} plane parallel to the polarized hydroxyapatite substrates on both negatively and positively charged surfaces due to the electrostatic force applied to the precipitated ions which accumulated

on the surface of the substrates [32]. The electric field plays several roles during crystallization of vaterite nanostructures from the solutions in our study. At first, the high electric field makes the titrant carrying static charge and then splits the titrant to nano-beams by electrostatic forces due to the same charges it taken. Secondly, it provides an electrical field to make ion orientation in the solution and thus changes the crystallization characteristics of the precipitations, such as orientating depositions or changing morphologies and phases. The crystalline graphic characteristics of CaCO_3 under the electric field are described in Fig. 5. Crystallization of CaCO_3 from solution under electric field is illustrated in Fig. 5a. The characteristics of the crystallization of both vaterite and calcite are studied and documented [8]. The formation of a stern layer of Ca counterions favors the oriented nucleation of crystal faces consisting of only Ca atoms and the (0001) face of vaterite fits this criterion. The trigonal planar carbonate anions are oriented parallel to the (0001) face of calcite, whereas in vaterite, they are aligned perpendicular, and this later arrangement is equivalent to the orientation of the carboxylates in conjunction with Ca binding generates a two-layer subunit cell motif of the vaterite structure

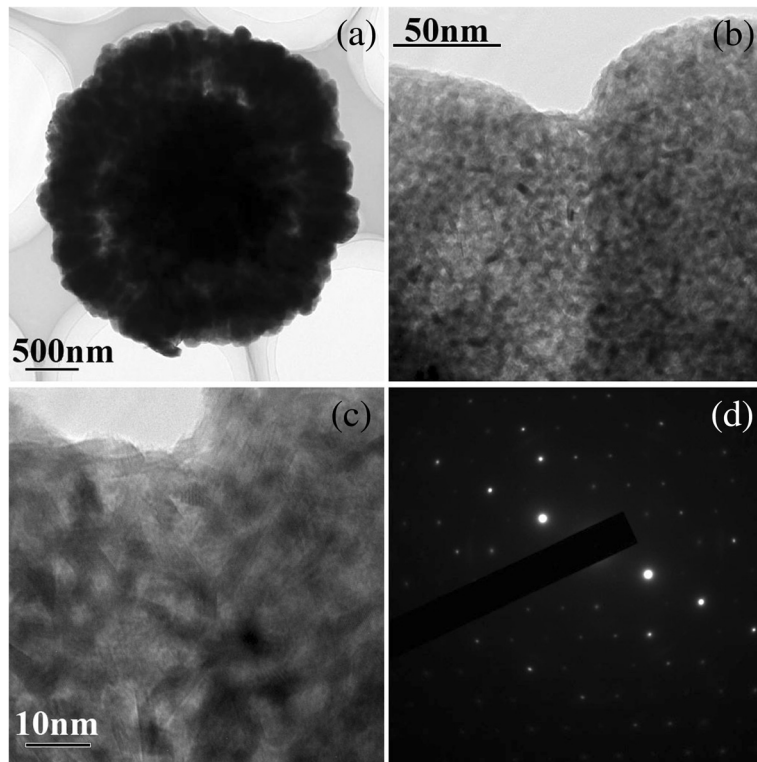


Fig. 4 TEM and SEAD pattern of sample EF, (a) a petaliform layer, (b) a conjunction of two nanorods, (c) detail structure of the conjunction, (d) SEAD pattern of the conjunction

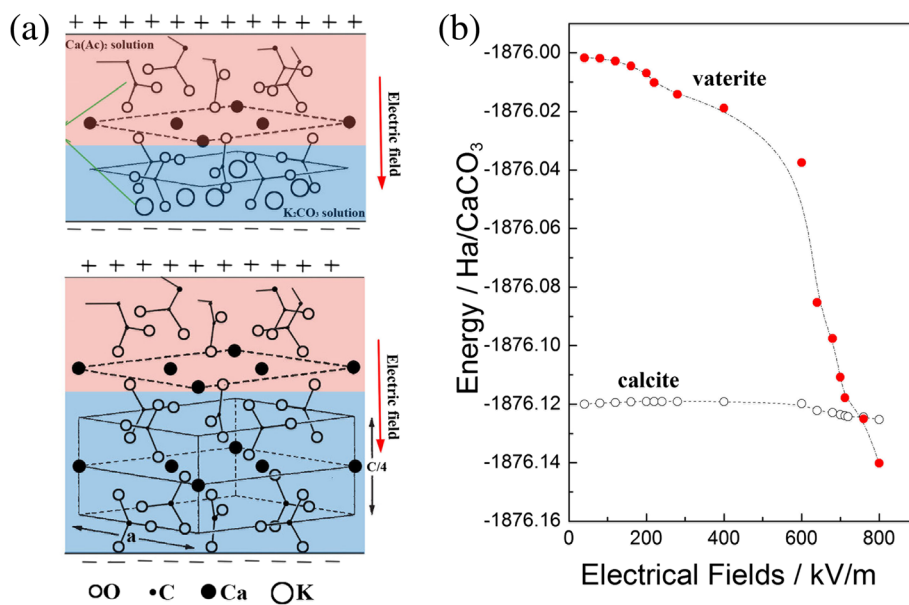


Fig. 5 The crystalline characteristics of CaCO_3 under the electric field. **a** Illustration of crystallization of CaCO_3 from solution under electric field [8]. **b** The dependence of energy of calcite and vaterite on electric field strength

rather than calcite. In our EF sample, the trigonal planar carbonate anions are aligned perpendicularly preferentially to a stern layer of Ca counter ions under the electric field, and vaterite crystal can be formed naturally.

To understand the transition between different polymorphs further, density functional theory (DFT) methods can enable itself as an extremely powerful tool for elucidating the energy changing of different polymorphs under electric field [33, 34]. The energy calculations are based on the Kohn-Sham equations which were derived from the Schrödinger equation. All calculations were performed with DMol3 package of Materials Studio. In the first step, the calculation models according to the crystallographic information file of calcite and vaterite were built, respectively. In the next, the energy of them under variable electric field within the density functional theory was calculated, where the exchange-correlation function has been parameterized according to the generalized gradient approximation in the Becke and Lee-yang-Parr function. The basis set “DND” was chosen and DFT Semi-core Pseudo pot was adopted for the core treatment of all atoms in the calculations. The tolerance of SCF is $<1.0-6$ eV. Satisfactory results were obtained and are shown in Fig. 5b. It can be seen that the energy of calcite (-1876.119947 Ha, 1 Ha = 27.2 eV) is lower than that of vaterite (-1876.001730 Ha), whereas the electric field is free, so that calcite is more stable and deposited from solution as the main crystal phase. The energy of both calcite and vaterite decreases with the increase of electric field strength, but the decrease rates of them are much different. The energy of calcite decreases with the electric field strength slowly; on the contrary, that of vaterite decreases speedily and drops down steeply at the electric field strength of about 500 kV/m, till the conversion appears at about 730 kV/m due to the energy of vaterite decreasing more quickly. All of these calculations are well consistent with our experimental results.

Conclusions

The electric field can be one of the most important factors to determine the polymorphs and morphology of the materials during their synthesis and their crystallization. It is found that the lattice structure and crystalline morphology can be tailored by the electric field which applied to the reaction system during deposition of CaCO_3 from solution. The calcite structure with cubic-like morphology can be obtained usually during deposition from solution. On the other hand, the vaterite structure with morphology of nanorod is formed under the high electric field. During crystallization of vaterites nanostructures from solutions, the electric field splits the titrant to nano-beams and provides an electrical field to make ions orientation in

solution and thus changes the crystallization characteristics of the precipitations. Both calculation and experiments confirmed that the electric field is propitious to the crystallization of vaterite during deposition from solution. The vaterite nanorods we synthesized under high electric field can be self-arranged into beautiful rose-like nanoflowers. The petal of rose-like nanoflowers is detected as mesocrystal, in which crystalline structures are constructed and/or transformed from larger units instead of single ions. Therefore, crystals can be assembled from nanoscopic building units in an almost perfect three-dimensional orientation to form so-called mesocrystals, exhibiting well-faceted outer surfaces.

Abbreviations

DFT: density functional theory; TEM: transmission electron microscopy; XRD: X-ray diffraction.

Competing interests

The authors declare that they have no competing interests.

Authors' contributions

JQQ contributed the idea and helped in the experimental designing. RG helped in the experiment executing. YW performed the experiment analysis. XLW helped in the material calculation. HLWC helped in the thesis direction. All authors read and approved the final manuscript.

Acknowledgements

The authors are grateful for the supports from the Basic Key Program of Applied Basic Research of Science and Technology Commission Foundation of Hebei Province in China (Grant No. 14961108D and Grant No. 15961005D) and Open Project of State Key Laboratory of New Ceramic and Fine Processing, Tsinghua University (No. KF201410).

Received: 22 December 2015 Accepted: 24 February 2016
Published online: 01 March 2016

References

1. Miller SL (1953) A production of amino acids under possible primitive earth conditions. *Science* 117:528–529
2. Iijima S (1991) Helical microtubules of graphitic carbon. *Nature* 354:56–58
3. Agarwal S, Wendorff HJ, Greiner A (2009) Progress in the field of electrospinning for tissue engineering applications. *Adv Mater* 21:3343–3351
4. Li D, Xia Y (2004) Electrospinning of nanofibers: reinventing the wheel? *Adv Mater* 16:1151–1170
5. Greiner A, Wendorff HJ (2007) Electrospinning: a fascinating method for the preparation of ultrathin fibers. *Angew Chem* 46:5670–5703
6. Stojilkovic A, Ishaque M, Justus U, Hamel L, Klimov E, Heckmann W, Eckhardt B, Wendorff HJ, Greiner A (2007) Preparation of water-stable submicron fibers from aqueous latex dispersion of water-insoluble polymers by electrospinning. *Polymer* 48:3974–3981
7. Wu H, Hu LB, Rowell MW, Kong D, Cha JJ, McDonough JR, Zhu J, Yang Y, McGehee MD, Cui Y (2010) Electrospun metal nanofiber webs as high-performance transparent electrode. *Nano Lett* 10:4242–4248
8. Mann S, Heywood BR, Rajam S, Birchall JD (1988) Controlled crystallization of calcium carbonate under stearic acid monolayers. *Nature* 334(25):692–695
9. Wang TX, Cölfen H, Antonietti M (2005) Mesocrystals and morphology change of CaCO_3 crystals in the presence of a polyelectrolyte additive. *J Am Chem Soc* 127:3246–3247
10. Xu AW, Antonietti M, Cölfen H, Fang YP (2006) Uniform hexagonal plates of vaterite CaCO_3 mesocrystals formed by biomimetic mineralization. *Adv Funct Mater* 16:903–908
11. Zhan JH, Lin HP, Mou CY (2003) Biomimetic formation of porous single-crystalline CaCO_3 via nanocrystal aggregation. *Adv Mater* 15:621–623
12. Marentette JM, Norwig J, Stockelmann E, Meyer WH, Wegner G (1997) Crystallization of CaCO_3 in the presence of PEO-block-PMAA copolymers. *Adv Mater* 9:647–651

13. Gebauer D, Cölfen H, Verch A, Antonietti M (2009) The multiple roles of additives in CaCO_3 crystallization: a quantitative case study. *Adv Mater* 21:435–439
14. Begum G, Rana RK (2012) Bio-inspired motifs via tandem assembly of polypeptides for mineralization of stable CaCO_3 structures. *Chem Commun* 48:8216–8218
15. Tsuzuki T, Pethick K, McCormick PG (2000) Synthesis of CaCO_3 nanoparticles by mechanochemical processing. *J Nanoparticle Res* 2:375–380
16. Oganov AR, Glass CW, Ono S (2006) High-pressure phases of CaCO_3 : crystal structure prediction and experiment. *Earth and Plan Sci Lett* 241:95–103
17. Popescu DC, Smulders MJ, Pichon BP, Chebotareva N, Kwak SY, Asselen Otto LJV, Sijbesma RP, DiMasi E, Sommerdijk AJM (2007) Template adaptability is key in the oriented crystallization of CaCO_3 . *J Am Chem Soc* 129:14058–14067
18. Rautaray D, Ahmad A, Sastry M (2003) Biosynthesis of CaCO_3 crystals of complex morphology using a fungus and an actinomycete. *J Am Chem Soc* 125:14656–14657
19. Naka K, Tanaka Y, Chujo Y (2002) Effect of anionic starburst dendrimers on the crystallization of CaCO_3 in aqueous solution: size control of spherical vaterite particles. *Langmuir* 18:3655–3658
20. Meldrum FC (2003) Calcium carbonate in biomineralisation and biomimetic chemistry. *Int Mater Rev* 48:187–224
21. Kato T, Sugawara A, Hosoda N (2002) Calcium carbonate–organic hybrid materials. *Adv Mater* 14:869–877
22. Avella M, Errico ME, Martuscelli E (2001) Novel PMMA/ CaCO_3 nanocomposites abrasion resistant prepared by an in situ polymerization process. *Nano Lett* 1:213–217
23. Xie XL, Liu QX, Kwok R, Li Y, Zhou XP, Zhang QX, Yu ZZ, Mai YW (2004) Rheological and mechanical properties of PVC/ CaCO_3 nanocomposites prepared by in situ polymerization. *Polymer* 45:6665–6673
24. Qi JQ, Sun L, Guo R, Li LT, et al. A chemical reaction device under electric field. Chinese patent, CN.201310667807.6, 2013.
25. Shiratori Y, Pithan C, Dornseiffer J (2007) Raman scattering studies on nanocrystalline BaTiO_3 (I)—isolated particles and aggregates. *J Raman Spectrosc* 38:1288–1299
26. Qi JQ, Peng T, Hu YM, Sun L, Wang Y, Chen WP, Li LT, Nan CW, Chan W, Lai H (2011) Direct synthesis of ultrafine tetragonal BaTiO_3 nanoparticles at room temperature. *Nanoscale Res Lett* 6:466
27. Simpson LJ (1998) Electrochemically generated CaCO_3 deposits on iron studied with FTIR and Raman spectroscopy. *Electrochim Acta* 43:2543–2547
28. Pierre MDL, Carteret C, Maschio L, André E, Orlando R, Dovesi R (2014) The Raman spectrum of CaCO_3 polymorphs calcite and aragonite: a combined experimental and computational study. *J Chem Phys* 140:164509–164520
29. Dandeu A, Humbert B, Carteret C, Muhr H, Plasari E, Bossoutrot JM (2006) Raman spectroscopy—a powerful tool for the quantitative determination of the composition of polymorph mixtures: application to CaCO_3 polymorph mixtures. *Chem Eng Technol* 29:221–225
30. Shevchenko EV, Talapin DV, Rogach AL, Kornowski A, Haase M, Weller H (2002) Colloidal synthesis and self-assembly of $\text{CoPt}(3)$ nanocrystals. *J Am Chem Soc* 124:11480–11485
31. Wohlrab S, Pinna N, Antonietti M, Cölfen H (2005) Polymer-induced alignment of DL-alanine nanocrystals to crystalline mesostructures. *Chem Eur J* 11:2903–2913
32. Wada N, Tanaka Y, Nakamura M, Kanamura K, Yamashita K (2009) Controlled crystallization of calcite under surface electric field due to polarized hydroxyapatite ceramics. *J Am Ceram Soc* 92:1586–1591
33. Wiberg KB, Stratman RE, Frisch MJ (1998) A time-dependent density functional theory study of the electronically excited states of formaldehyde, acetaldehyde and acetone. *Chem Phys Lett* 297:60–64
34. Guo R, Liu F, Zhang B et al (2014) Synthesis, structures, properties and DFT studies of two Ni(II) complexes with pyridine-3, 5-dicarboxylic acid. *Chin J Inor Chem* 30:1635–1640.

Submit your manuscript to a SpringerOpen® journal and benefit from:

- Convenient online submission
- Rigorous peer review
- Immediate publication on acceptance
- Open access: articles freely available online
- High visibility within the field
- Retaining the copyright to your article

Submit your next manuscript at ► springeropen.com
